

IES Standards for Electromagnetic Quality Measurement

Lazar Sladojevic, Lidija Korunovic, Miodrag Stojanovic and Vladeta Milenkovic
Lazar Sladojevi is with the Faculty of Electronic Engineering at University of Niš
Aleksandra Medvedeva 14
18000 Niš, Serbia
{lazar.sladojevic@elfak.rs}
{lidija.korunovic@elfak.ni.ac.rs}
{miodrag.stojanovic@elfak.ni.ac.rs}
{vladeta.milenkovic@elfak.ni.ac.rs}



ABSTRACT: *The standards for electromagnetic compatibility and quality is IEC protocols. For power quality observation, a set of algorithms for supply assessment is used to study the voltage imbalance. The coding used is Python, and it is assessed based on real signals. The outcome is analysed and described with inferences, and some results are discussed.*

Keywords: Voltage Unbalance, IEC 61000-4-30, Power Quality, Python

Received: 28 November 2022, Revised 5 February 2023, Accepted 18 February 2023

DOI: 10.6025/jio/2023/13/2/35-42

Copyright: with authors

1. Introduction

Power quality (PQ) is becoming increasingly important problem in electrical power systems. The deviation of supplying voltage from the ideal sine wave in many areas is now evident more than ever. This is most obvious in the areas with extensive usage of electronic devices. These devices generate higher order harmonics which impact negatively the supplying power grid, thus generating additional power and energy losses [1].

There is a total number of twelve power quality parameters defined in the IEC 61000 Standard for Electromagnetic compatibility, part 4-30 which considers Power quality measurement methods that should be addressed, measured and evaluated [2]. The standard defines measurement methods as well as measurement uncertainty and measurement range for each individual parameter, except for measurement of flickers, harmonics and interharmonics, which are described in separate standards. Two classes of measurement equipment are recognized, class *A* and class *S* and the main difference between them is the accuracy - class *A* is more accurate than class *S*.

This paper addresses the problem of real-time measurement of supplying voltage unbalance. Voltage unbalance can occur for

different reasons. For example, it can be caused by unbalanced load or by the supplying grid itself [3]. As a result, huge losses in electrical drives can be observed [4]. Unlike some other power quality parameters such as voltage dips and swells, small unbalance usually doesn't produce immediate negative effects, but rather has long term consequences [5].

For the measurement of unbalance, a data acquisition platform has been developed and used in conjunction with fast ARM processor for the necessary calculations. Unbalance measurement algorithm was entirely written in Python programming language. The goal is to achieve real time evaluation of voltage unbalance and to present the results of practical implementation of the methods proposed in standard IEC 61000-4-3.

2. Parameter Description and Calculation Methods

Supply voltage unbalance is a state of voltage waveforms in a three-phase system which deviates from the ideal model. The ideal model is characterized by three pure sine wave voltages with the rated magnitude and frequency whose phasors are angularly displaced from each other by 120 degrees. Therefore, voltage unbalance can either be influenced by different magnitudes of the voltages or by phase shifts that deviate from those of ideal model.

There are different methods for calculation of voltage unbalance [6]. According to IEC 1000-3-x series standards, the unbalance is calculated using the method of symmetrical components. This method is well known in electrical engineering and it is based on fact that every unbalanced (asymmetrical) three-phase system can be mathematically represented by the superposition of three balanced three-phase systems. These three systems are called the direct sequence system, the inverse sequence system and the zero sequence system, and have the same frequency as the original system. Assuming that phase *A* is the referent voltage phase, phase *B* lags by 120 degrees and phase *C* by 240 degrees relative to phase *A* in direct sequence system, while in the inverse system phases *B* and *C* lead by the same angles. In zero sequence system, there is no phase shift among voltage waveforms. Each phase phasor is a vector sum of corresponding direct, inverse and zero component.

The IEC standards define that the voltage unbalance is evaluated by the so-called Voltage Unbalance Factor (*VUF*). This factor represents ratio of the magnitudes of inverse sequence and direct sequence fundamental components of voltage, expressed in percent,

$$VUF = u_2 = \frac{U^i}{U^d} \cdot 100 \quad (1)$$

In Equation 1, U^i is the magnitude of inverse sequence component of fundamental voltage, U^d is the magnitude of direct sequence component of fundamental voltage, and u_2 is the alias for *VUF* which is used in IEC 61000-4-30 Standard. In standards defining the maximum allowed voltage unbalance in transmission and distribution grid, these limits are given as maximum values of *VUF*.

On the other hand, ANSI and IEEE standards present the methods for voltage unbalance calculation that do not take into account the irregular phase shifts. They observe only the changes in magnitudes. Thus, the IEC method defined in IEC 61000-4-30 Standard is used in this paper for the calculation of voltage unbalance.

3. Algorithm Description

IEC 61000-4-30 Standard defines that the sliding 10 cycles window is used for unbalance calculation in 50 Hz systems. This means that unbalance *VUF* factor, Equation 1, is calculated approximately every 200 ms. There are no requirements for the synchronization of this window with zero cross points of any of the phases, like for example in the case of voltage dips, swells and interruption detection. The accuracy class A of the standard states that measurement uncertainty for unbalance *VUF* factor value is equal to 0.15%.

The detection method described above implicitly requires two things: fundamental magnitude calculation and fundamental cycle duration calculation. The fundamental magnitude calculation refers to calculation of magnitude of the fundamental component of voltage wave, i.e. component on the fundamental frequency in spectrum. This is necessary because voltage can also contain higher order harmonics which need to be minimized before the calculations. There are two ways to minimize

higher order harmonics, as recommended by standard: the filtration using low pass filter or the Discrete Fourier Transform (DFT). The modification of the latter kind is applied in this paper. Namely, the corresponding algorithm uses the Python's built-in Fast Fourier Transform (FFT), which is a faster, optimized version of the DFT [7]. As required by the standard, the FFT is executed over each 10 cycles window.

Fundamental cycle duration is expressed as a number of samples N in one full cycle. This number can be calculated from the frequency of signal, f , and the sampling frequency, f_s :

$$N = \text{round} \left(\frac{f_s}{f} \right) \quad (2)$$

There are number of frequency estimation methods, some of those are explained in detail in [8–11], but for the application presented in this paper, a simple zero-crossing detection method is used. This method uses the linear regression over the samples around the first and the last zero cross of a signal. Samples involved in the linear regression are the ones with values between the fixed upper and lower threshold. This way, a variable number of samples is used for each linear regression, because the signal always contains some noise. This noise can cause multiple zero crosses and non-equal number of positive and negative samples. Here, linear regression behaves as some type of a filter, because it constructs the straight line which minimizes the sum of squared distances from all samples involved in regression,

$$\min \sum_{i=1}^M (U_i - \hat{U}_i)^2 = \min \sum_{i=1}^M (U_i - (a \cdot t_i + b))^2 \quad (3)$$

In Equation 3, \hat{U}_i is the projection of sample U_i on the regression line, M is number of samples involved in linear regression, a is the line slope coefficient, b is line intercept coefficient, and t_i is the time point at which the sample was taken.

The approach is fairly simple and computationally effective, but can give errors when applied to highly distorted signals. In these cases, IEC 61000-4-30 Standard recommends filtration of a signal before the estimation of its frequency. However, primary goal of this paper is developing and evaluation of practical algorithm for voltage unbalance measurement, and for simplicity, that will be done on fairly clean, sine waveform signals. This assumption is not always fulfilled in practice, but processing of highly distorted signal requires better frequency measurement, and will be the subject of authors' future work. Nevertheless, the algorithm is not influenced significantly by harmonic distortion, since the calculations are performed on fundamental components of signals which are extracted from FFT.

4. Experimental Results

For experimental purposes, a data acquisition and processing platform has been developed. The platform contains 16-bit Analog to Digital (A/D) converter with the 25.6 kHz sampling frequency for data acquisition and ARM Cortex-A8 AM335X microprocessor for digital processing of the gathered data. Platform is capable of sampling and processing of all three voltage channels simultaneously.

The algorithm itself was entirely written in Python programming language. Python was chosen because it is simple and open source programming language, yet very powerful when it comes to scientific computing. Python runs on Linux operating system which is embedded in the platform. The algorithm was developed to comply with class A measurement instrumentation. Sets of sampled data from each voltage channel are received in the packages of 25600 samples, which means they are sampled for one second before they are processed. This implies that the algorithm has to process the whole previous set of samples in time period shorter than one second, i.e. before the new samples are received. Therefore, the algorithm has to be highly optimized.

For test voltage generation, Omicron CMC 356 test set was used [12]. This test set is primarily designed for relay protection testing, but it can also serve well other purposes, such as the one described in this paper.

Many test cases have been created and examined, but only a part of the results is shown due to lack of space. Five characteristic cases are depicted in Figures. 1 to 5. The overview of the results is given in Table I, while the processing times for one-second data buffers are presented in Table 2. Besides voltage unbalance measurements, signal frequency is estimated and

FFT calculations are conducted each second. FFT is performed over 10 cycle time interval and fundamental phasor is extracted. All three phases' phasors are then used in Equation 4 to derive symmetrical components for that time period.

$$\begin{bmatrix} U^d \\ U^i \\ U^0 \end{bmatrix} = \frac{1}{3} \begin{bmatrix} 1 & a & a^2 \\ 1 & a^2 & a \\ 1 & 1 & 1 \end{bmatrix} \cdot \begin{bmatrix} U_{AN} \\ U_{BN} \\ U_{CN} \end{bmatrix} \quad (4)$$

In Equation 4, U^d , U^i and U^0 are the phase A direct, inverse and zero sequence components, respectively, U_{AN} , U_{BN} , U_{CN} are phase-to-neutral voltage magnitudes for phase A, B and C, respectively, and $a = e^{j.2\pi/3}$. Besides VUF, a similar zero-sequence factor is also requested by standard IEC 61000-4-30:

$$u_0 = \frac{U^0}{U^d} \cdot 100 \quad (5)$$

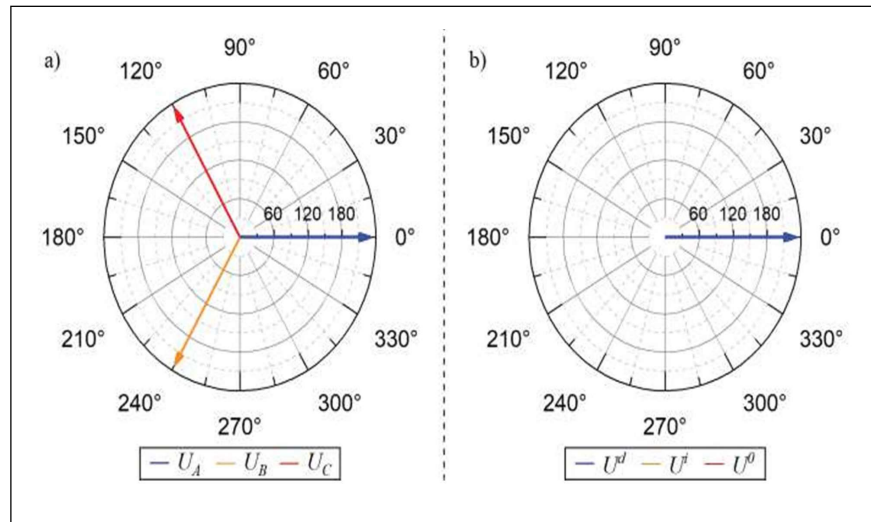


Figure 1. Test case 1 a) phasors and b) symmetrical components

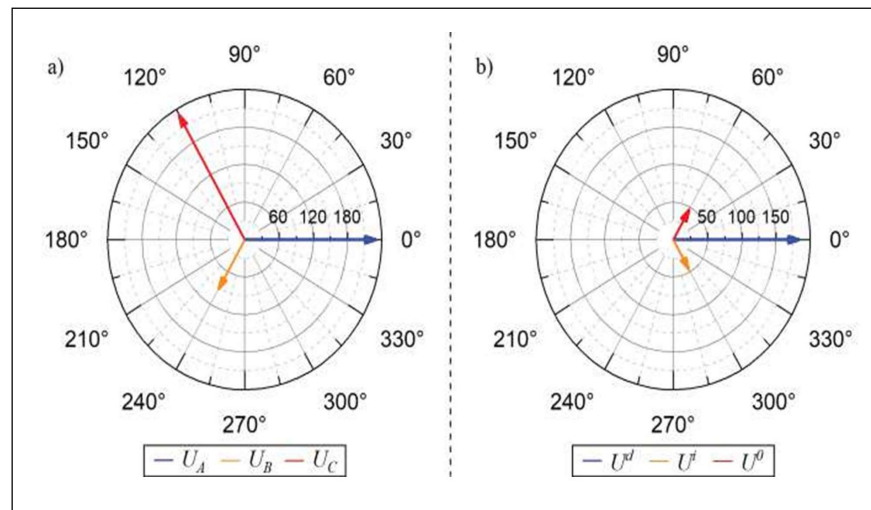


Figure 2. Test case 2 a) phasors and b) symmetrical components

Test case index	1	2	3	4	5
U_{A-fund} [V]	230 $\angle 0^\circ$	230 $\angle 0$	230 $\angle 0$	230 $\angle 0$	230 $\angle 0$
U_{B-fund} [V]	230 $\angle -120^\circ$	92 $\angle -120^\circ$	230 $\angle -120^\circ$	230 $\angle -120^\circ$	92 $\angle -90^\circ$
U_{C-fund} [V]	230 $\angle 120^\circ$	230 $\angle 120^\circ$	92 $\angle 120^\circ$	230 $\angle 90^\circ$	92 $\angle 90^\circ$
U_{real}^d [V]	230 $\angle 0^\circ$	184 $\angle 0^\circ$	184 $\angle 0^\circ$	223 $\angle -9.9^\circ$	129.766 $\angle 0^\circ$
U_{real}^i [V]	0 $\angle 0^\circ$	46 $\angle -60^\circ$	46 $\angle 60^\circ$	39.6842 $\angle 135^\circ$	23.552 $\angle 0^\circ$
U_{real}^0 [V]	0 $\angle 0^\circ$	46 $\angle 60^\circ$	46 $\angle -60^\circ$	39.6842 $\angle 15^\circ$	76.682 $\angle 0^\circ$
$U_{estimated}^d$ [V]	229.985 $\angle 0.01^\circ$	183.976 $\angle -0.01^\circ$	183.9899 $\angle -0.01^\circ$	223.0314 $\angle -9.88^\circ$	129.776 $\angle -0.01^\circ$
$U_{estimated}^i$ [V]	0.057 $\angle -111.3^\circ$	45.949 $\angle -60.06^\circ$	46.0208 $\angle 60.06^\circ$	39.6804 $\angle 135.1^\circ$	23.5613 $\angle 0.04^\circ$
$U_{estimated}^0$ [V]	0.019 $\angle 35.83^\circ$	46.0004 $\angle 60.02^\circ$	45.9845 $\angle -60.05^\circ$	39.6592 $\angle 15.01^\circ$	76.668 $\angle -0.04^\circ$
u_{2-real}	0	25	25	17.7913	18.1496
u_{0-real}	0	25	25	17.7913	59.0925
$u_{2-estimated}$	0.025	24.9756	25.0127	17.7914	18.1554
$u_{0-estimated}$	0.0083	25.0034	24.9930	17.7819	59.0774
u_2 estimation error [%]	0.025	0.0244	0.0127	0.0001	0.0058
u_0 estimation error [%]	0.0083	0.0035	0.0070	0.0094	0.0152

Table 1. Parameters of Test Cases

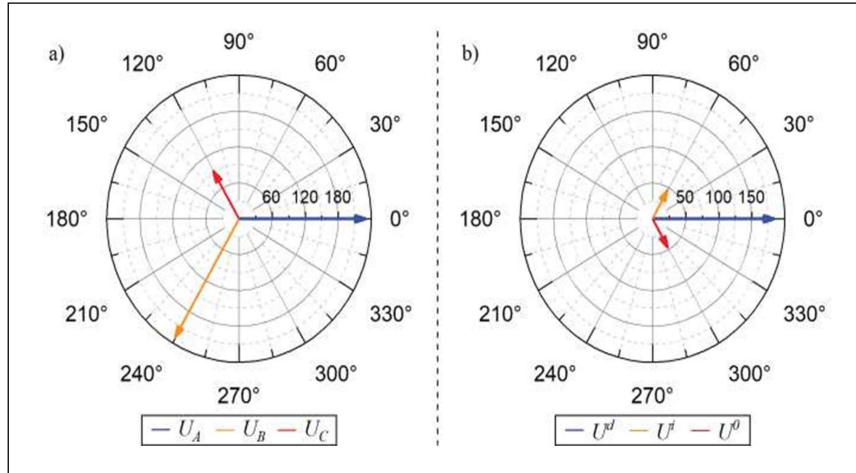


Figure 3. Test case 3 a) phasors and b) symmetrical components

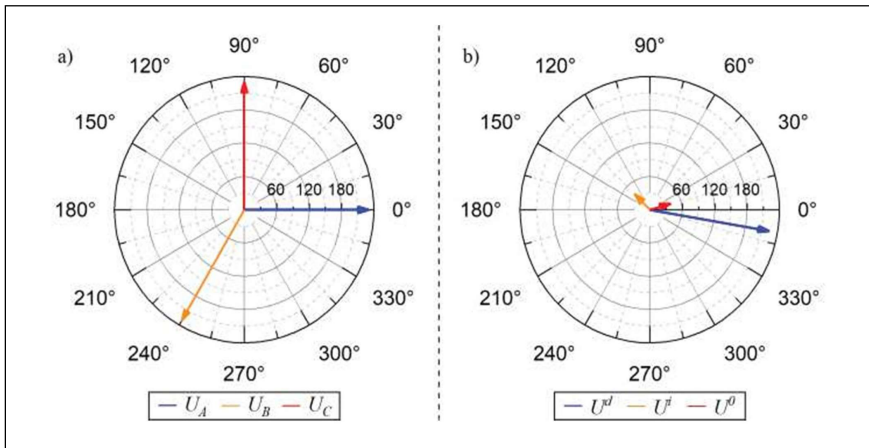


Figure 4. Test case 4 a) phasors and b) symmetrical components

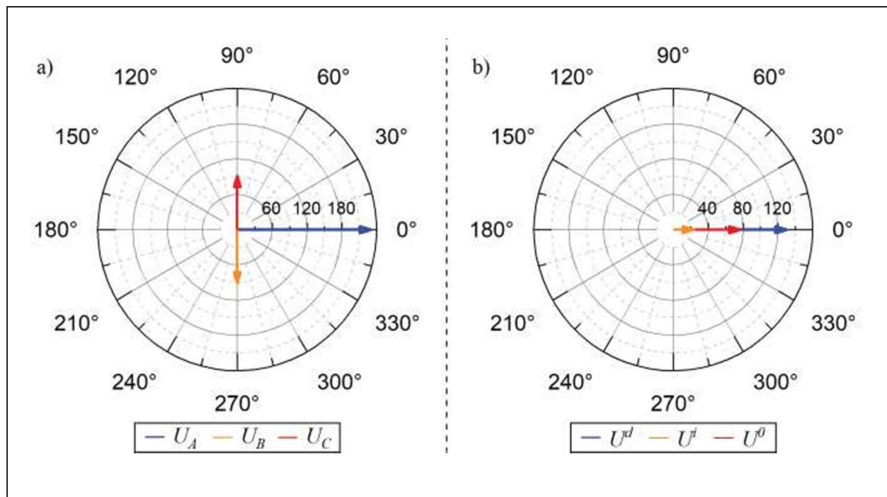


Figure 5. Test case 5 a) phasors and b) symmetrical components

Each figure shows all three phases' phasors on the left side and measured symmetrical components on the right side. The values indexed as *real* in Table I are directly read from Omicron test software and these are the correct parameters of actually produced signals. Values for $u_{2-estimated}$ and $u_{0-estimated}$ are 150 cycles aggregated values whose calculation is mandatory for class A equipment. Note that presented cases are the most extreme ones (some of them are also considered voltage dips), but it is known that the algorithms are most efficiently tested in extreme conditions.

Last two rows in Table 1. are the most important. They present absolute values of measurement errors for u_2 (*VUF*) and u_0 . It is obvious that none of these values is greater than 0.15 %, which is class A uncertainty limit as described in applied standard. Similar values are obtained from other test cases, which are not presented here. Further, Table 2. shows that the average calculation time is shorter than one second, which is time available for processing of one buffer of data. This proves that the algorithm is well designed and capable of real-time class A voltage unbalance measurement.

5. Conclusions

In this paper the software algorithm for measurement of supply voltage unbalance is presented. The goals of algorithm are to achieve real time measurement performance of this abnormal state in power systems, and to evaluate practically obtained results applying the method described in standard IEC 61000-4-30. For practical purposes, new data acquisition platform is developed and tested. Five test cases are examined and experimental results are presented. It can be concluded that the proposed algorithm is capable of real-time voltage unbalance measurements with very high precision which complies with class A instrumentation.

Test case index	Average processing time for one buffer of data [s]
1	0.8211
2	0.8205
3	0.8194
4	0.8254
5	0.8257

Table 2. Processing Times For Different Test Cases

In this paper clean sinusoidal voltages are examined, whereas further results will be obtained taking into account the presence of higher order harmonics. The research in this field and the improvement of developed algorithm will be the subject of authors' future papers.

Acknowledgement

This research is partly supported by project grant III44006 financed by the Ministry of education, science and technology development of the Republic of Serbia.

References

- [1] Dugan, R., McGranaghan, M., Santoso, S. and Beaty, H. (2004). *Electrical Power Systems Quality*, Second edition, McGraw-Hill, 2004.
- [2] *IEC 61000 International Standard – Electromagnetic Compatibility, Part 4-30: Testing and Measurement Techniques, - Power Quality Measurement Methods*, edition 3.0, 2015.
- [3] Pierrat, L. and Morrison, R.E. (1995). Probabilistic Modeling of Voltage Asymmetry, *IEEE Trans. on Power Delivery*, 10 (3),

pp 1614-1620, July.

- [4] Kostic, M. and Nikolic, A. (2010). Negative Consequence of Motor Voltage Asymmetry and Its Influence to The Unefficient Energy Usage, *WSEAS Trans. on Circuits and Systems*, Issue 8, Volume 9, Aug. 2010.
- [5] Valois, P.V.S., Vieira Tahan, C.M., Kagan, N. and Arango, H. (2001). Voltage Unbalance in Low Voltage Distribution Networks, 16th International Conference and Exhibition on Electricity Distribution, 2001. Part 1: Contributions. CIRED. (IEE Conf. Publ No. 482), June.
- [6] Albadi, M.H., Al Hinai, A.S., Al-Badi, A.H., Al Riyami, M.S., Al Hinai, S.M. and Al Abri, R.S. (2015). Unbalance in Power Systems: Case Study, 2015 *IEEE International Conference on Industrial Technology (ICIT)*, Seville, Spain, 2015. p 1407-1411. DOI: [10.1109/ICIT.2015.7125294](https://doi.org/10.1109/ICIT.2015.7125294)
- [7] Cooley, J.W. and Tukey, J.W. (1965). An Algorithm for the Machine Calculation of Complex Fourier Series, *Math. Comput.* 19: 297-301, April 1965.
- [8] Sachdev, M.S. and Giray, M.M. (1985). A Least Error Squares Technique for Determining Power System Frequency, *IEEE Trans. Power App. Syst.*, vol. PAS-104, 2, p 437-444, February 1985.
- [9] Karimi, H., Karimi-Ghartemani, M. and Iravani, M.R. (2004). Estimation of Frequency and Its Rate of Change for Applications in Power Systems, *IEEE Trans. Power Del.*, 19 (2) p. 472-480, April 2004.
- [10] Djuric, M.B. and Djurišić, Ž.R. (2008). Frequency Measurement of Distorted Signals Using Fourier And Zero Crossing Techniques, *Electric Power Systems Research* Volume 78, Issue 8, p 1407-1415, Aug. 2008.
- [11] Lavopa, E., Zanchetta, P., Sumner, M. and Cupertino, F. (2009). Real- Time Estimation of Fundamental Frequency and Harmonics for Active Shunt Power Filters in Aircraft Electrical Systems, *IEEE Trans. on Industrial Electronics*, Vol. 56, No. 8, pp. 2875-2884, August 2009.
- [12] CMC. CMC356.ae, 356 Reference Manual, Article Number VESD2003 - Version, 4.